Journal of
**Synchrotron Radiation**

ISSN 0909-0495

Received 1 August 2007
Accepted 10 December 2007

# Solution structures of RseA and its complex with RseB

**Kyeong Sik Jin,[a]‡ Dong Young Kim,[b]‡ Yecheol Rho,[a] Van Binh Le,[b] Eunju Kwon,[b] Kyeong Kyu Kim[b]* and Moonhor Ree[a]***

[a]Department of Chemistry, National Research Laboratory for Polymer Synthesis and Physics, Pohang Accelerator Laboratory, Center for Integrated Molecular Systems, Polymer Research Institute, and BK School of Molecular Science, Pohang University of Science and Technology (Postech), Pohang 790-784, Republic of Korea, and [b]Department of Molecular Cell Biology, Samsung Biomedical Research Institute, Sungkyunkwan University School of Medicine, Suwon 440-746, Republic of Korea. E-mail: kkim@med.skku.ac.kr, ree@postech.edu

The bacterial envelope stress response, which is responsible for sensing stress signals in the envelope and for turning on the $\sigma^E$-dependent transcription, is modulated by the binding of RseB to RseA. In this study, the solution structures of RseA and its complex with RseB were analyzed using circular dichroism and small-angle X-ray scattering. The periplasmic domain of RseA is unstructured and flexible when it is not bound to RseB. However, upon the formation of the stable complex with RseB, RseA induces conformational changes in RseB and, at the same time, RseA becomes more structured. Furthermore, it appears that some other undefined region of RseA, as well as the previously identified minimum region (amino acid 169–186), is also involved in RseB binding. It is thought that these conformational changes are relevant to the proteolytic cleavage of RseA and the modulation of envelope stress response.



**Keywords: $\sigma^E$ signaling pathway; envelope stress response; RseA; RseB; small-angle X-ray scattering; circular dichroism.**

## 1. Introduction

RseA/$\sigma^E$ signalling has been intensively studied as one of the envelope stress responses in Gram-negative bacteria (Alba & Gross, 2004). Various stress signals, detected *via* the increase in unfolded OMP peptide in the extracytoplasmic compartment, are transduced into the cytoplasmic compartment through the periplasmic membrane (Alba *et al.*, 2002; Kanehara *et al.*, 2002; Walsh *et al.*, 2003; Flynn *et al.*, 2004) and thus activate the genes required for the defence or recovery of the cells against the stress (Rhodius *et al.*, 2006). The periplasmic domain of RseA is cleaved by the activated DegS in stress conditions (Walsh *et al.*, 2003; Wilken *et al.*, 2004) and, following this cleavage, the cytoplasmic domain of RseA is digested by RseP. This sequential digestion of RseA results in the release of $\sigma^E$, which ultimately enhances the transcription of the gene involved in stress response (Alba *et al.*, 2002; Kanehara *et al.*, 2002). RseB prevents the proteolytic cleavage of RseA by binding to the periplasmic region of RseA (Missiakas *et al.*, 1997; Grigorova *et al.*, 2004). It is thought that the role of RseB is essential for the negative regulation of $\sigma^E$ signalling, since RseP alone can cleave RseA in a cell in which RseB and DegS are null-mutated (Grigorova *et al.*, 2004). RseB has also been proposed to activate the function of $\sigma^E$ by sensing other stress signals, including damaged proteins in periplasmic space. Therefore, it is considered that RseB functions for the fine tuning of the $\sigma^E$ envelope stress response by modulating the activity of RseP (Grigorova *et al.*, 2004).

Recent crystal structure analysis of RseB and its binding with RseA provided the framework for understanding the role of RseB (Kim *et al.*, 2007). RseB is composed of two domains and forms a loosely packed dimer with two grooves on each side. In RseA, the residues 169–186 were identified as the minimum region required for RseB binding. The conserved negatively charged region in RseB is expected to be important in this binding. It was also proposed, on the basis of small-angle X-ray scattering (SAXS) studies of RseB and its complex with RseA (Kim *et al.*, 2007), that the periplasmic domain of RseA ($RseA_{121–216}$) binds to the groove of the RseB dimer and induces conformational changes in RseB. However, it is not yet clearly known how RseA binds to RseB in solution, and how their binding modulates the proteolytic activity of RseP and, ultimately, the envelope stress response.

We have analyzed the conformations of RseA and its complex with RseB using solution SAXS and observed conformational alterations induced by the formation of the complex. These results reveal that their binding induces conformational changes in both RseA and RseB, and will provide necessary information for understating the regulation mechanism of proteolytic cleavage of RseA.

## 2. Materials and methods

### 2.1. Sample preparation

Recombinant RseB and RseA used in our studies were expressed and purified in buffer *A* (20 m*M* Tris–HCl pH 7.5 and 100 m*M* NaCl) as described previously (Kim *et al.*, 2007). The periplasmic domain of

‡ K. S. Jin and D. Y. Kim contributed equally to this work.

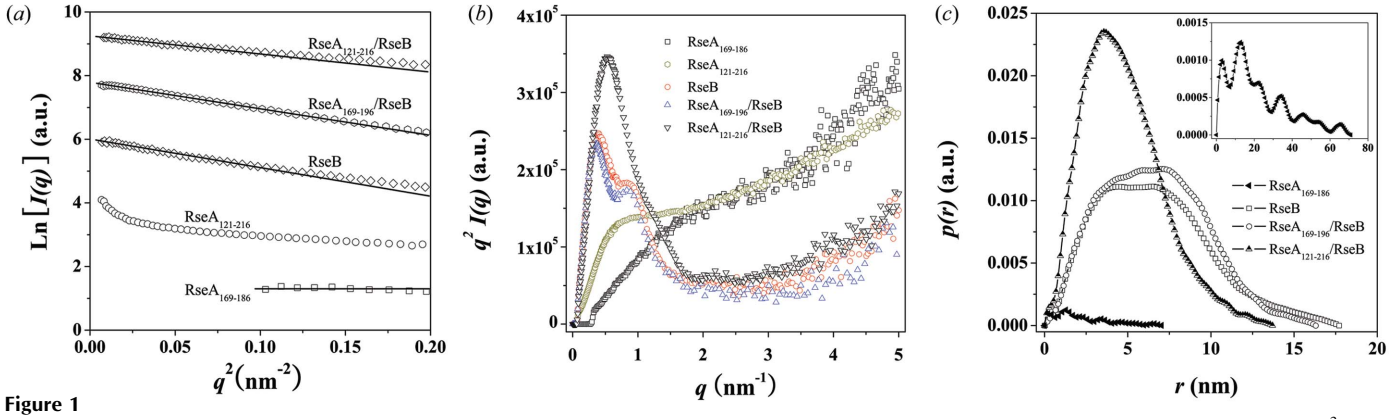


**Figure 1**
Experimental SAXS data for RseB, $RseA_{121–216}$, $RseA_{169–186}$, $RseA_{121–216}$/RseB and $RseA_{169–196}$/RseB are depicted by (*a*) Guinier plots and (*b*) Kratky plots along $q^2$ and $q$, respectively. Each plot is shifted along the vertical axis for clarity. (*c*) The distance distribution function $p(r)$ of each protein was obtained from the experimental SAXS data. The plot of $RseA_{169–196}$ is drawn in the upper right panel in magnified scale.

RseA ($RseA_{121–216}$) and the truncated RseA containing the minimum binding region ($RseA_{169–196}$) were prepared using metal affinity chromatography, thrombin treatment and gel filtration chromatography in buffer *A*. The minimal RseB binding region of RseA ($RseA_{169–186}$) was synthesized by EZBiolab Inc. (USA).

### 2.2. SAXS data collection and analysis

The SAXS data were collected at the SAXS beamline 4C1 (Bolze *et al.*, 2002; Yu *et al.*, 2005; Jang *et al.*, 2006) of Pohang Light Source, Republic of Korea. The scattering of proteins in the concentration range 2–20 mg ml$^{-1}$ was measured at 298 K at a wavelength of $\lambda$ = 1.608 Å, using a two-dimensional charge-coupled detector (MAR165, USA) in the scattering range $0.15 < q < 5$ nm$^{-1}$ ($q = 4\pi\sin\theta/\lambda$, where $2\theta$ is the scattering angle). Each measurement was collected for 1 min. Each dimensional (2D) SAXS pattern was circular averaged from the beam center, then normalized to the transmitted X-ray beam intensity, which was monitored with a scintillation counter placed behind the sample, and corrected for the scattering due to the buffer solution. The optimal concentration of proteins, suitable for data processing, was 10 mg ml$^{-1}$.

The radius of gyration $R_g$ was determined by fitting the measured scattering data with the Guinier equation, $\ln I(q) = \ln I(0) - r_g^2 q^2/3$ at $qR_g < 1.3$ (Glatter, 1982; Jang *et al.*, 2006). The program *GNOM* (Semenyuk & Svergun, 1991) was used to compute the pair distance distribution function $p(r)$. To reconstruct the molecular shape of proteins in solution, *GASBOR*, an *ab initio* molecular shape determination program, was used (Svergun *et al.*, 2001). In total, ten models were generated and the most probable one was selected using the program package *DAMAVER* (Volkov & Svergun, 2003). The final models at 12.5 Å resolution were obtained by imposing a twofold symmetry restriction under the assumption that RseB exists as a dimer. The crystal structure of RseB used for structure comparison was obtained from the Protein Data bank (PDB code of *E. coli* RseB: 2p4b).

### 2.3. CD spectroscopy

The protein samples for circular dichroism (CD) analyses were prepared in buffer *A*. CD spectra were obtained at 277 K using a Jasco J-815 CD spectrometer. The scans were collected at 1 nm intervals with a scanning speed of 10 nm min$^{-1}$ over the wavelength range 190–250 nm. The spectra resulting from the accumulation of three scans were smoothed and normalized to molar ellipticity using the mean weight residue.

## 3. Results and discussion

### 3.1. SAXS analysis of RseAs and their complexes with RseB

The crystal structure and the solution SAXS structure of RseB revealed the flexibility of the conformation of RseB and indicated that RseB may undergo conformational changes upon RseA binding (Kim *et al.*, 2007). To elucidate the solution structure of RseA and its binding mode to RseB, more SAXS experiments were performed using the periplasmic domain and the minimum RseB binding region of RseA ($RseA_{121–216}$ and $RseA_{169–186}$, respectively), RseB, and their complexes ($RseA_{121–216}$/RseB and $RseA_{169–196}$/RseB). $RseA_{169–196}$ was used for complex formation instead of $RseA_{169–186}$, since it showed higher binding affinity to RseB.

The Guinier plots of the measured SAXS data revealed various conformational forms of truncated RseAs, RseB and RseA/RseB complexes (Fig. 1*a*). In the Guinier plots, except for $RseA_{121–216}$, each scattering curve is well fitted to a straight line, indicating that the protein is considerably homogeneous in terms of the conformation. The radius of gyration ($R_{g,G}$) was estimated from the slope value of the regression line within the Guinier region shown in Fig. 1(*a*). The determined $R_{g,G}$ values increase in the order $RseA_{169–186}$ < $RseA_{121–216}$/RseB < RseB $\simeq$ $RseA_{169–196}$/RseB (Table 1). Interestingly, the $RseA_{121–216}$/RseB complex has a smaller $R_{g,G}$ value than the unbound RseB. This indicates that RseB is less flexible in the RseA-bound state than in the free state, which might be attributed to its conformation being fixed by the binding of RseA to the open grooves, as previously reported (Kim *et al.*, 2007). The scattering profile of $RseA_{121–216}$ showed a steep slope toward $q = 0$ (Fig. 1*a*), indicative of the presence of a large diversity in size and conformation, that is, the fully unstructured state of the periplasmic domain of RseA. In contrast, $RseA_{169–186}$ appears to be more homogeneous in conformation, which is probably a result of its small size.

In general, the scattering curve for a globular conformation follows Porod's law, $I(q) \propto q^{-4}$ in the large-$q$ region, whereas the scattering profile from an expanded unfolding conformation is proportional to $q^{-2}$ at moderate $q$, and is then proportional to $q^{-1}$ at small $q$ values (Glatter, 1982; Flanagan *et al.*, 1992; Kataoka *et al.*, 1993, 1995). Furthermore, the Kratky plot of the scattering curve for the globular structure shows a clear peak, whereas that of a molten globule has a plateau and then increases gradually with $q$ (Glatter, 1982; Flanagan *et al.*, 1992; Kataoka *et al.*, 1993, 1995). Thus, Kratky analysis was further carried out for the measured SAXS data in order to obtain more useful information on the folding status. The Kratky plots of the measured scattering data are shown in Fig. 1(*b*).

**Table 1**
Structural parameters obtained from the SAXS data of RseAs, RseB and RseA/RseB complexes.

| | $R_{g,G}$ (nm)† | $R_{g,p(r)}$ (nm)‡ | $D_{max}$ (nm)§ | Shape¶ |
|---|---|---|---|---|
| $RseA_{169–186}$ | 1.67 (10) | 1.90 (3) | 7.10 | Random chain |
| $RseA_{121–216}$ | – | – | – | Random chain |
| RseB | 5.07 (20) | 5.22 (1) | 17.70 | Globular |
| $RseA_{169–196}$/RseB | 5.14 (10) | 5.12 (1) | 16.30 | Globular |
| $RseA_{121–216}$/RseB | 3.67 (10) | 3.75 (1) | 13.70 | Globular |

† $R_{g,G}$ was calculated from the Guinier fit. ‡ $R_{g,p(r)}$ was calculated from the $p(r)$ function using the program *GNOM*. § $D_{max}$ was obtained from the $p(r)$ function using the program *GNOM*. ¶ Shape was determined from the Kratky plot and the $p(r)$ function.

As can be seen in Fig. 1(*b*), the Kratky plots of $RseA_{169–186}$ and $RseA_{121–216}$ do not show clear peaks but rapidly increase in the small-$q$ range ($0.3 < q < 1$ nm$^{-1}$). Then they gradually increase in intermediate- and high-$q$ regions (Fig. 1*b*). These plots clearly resemble that of a random-coil-like polymer with a certain degree of chain rigidity (Roe, 2000). Taking this fact into account, the Kratky analyses indicate that $RseA_{169–186}$ and $RseA_{121–216}$ have nearly random-coiled conformations with limited globularity.

In contrast, the distinct peaks shown in the Kratky curves of RseB and its complexes with RseAs in the small-$q$ region indicate that they form globular structures. The curves for RseB and $RseA_{169–196}$/RseB have two sharp peaks, which may originate from different orientations of two large N-terminal domains, presumably as a result of the open conformation of the RseB dimer in solution (Fig. 1*b*). In the case of the $RseA_{121–216}$/RseB complex, the Kratky plot has a well defined peak in the small-$q$ region. This result confirms that the binding of $RseA_{121–216}$ to RseB induces transformation of its overall structure, as shown in the above Guinier analysis.

### 3.2. Solution models and CD spectra of RseA and RseB proteins

Real-space information of the SAXS scattering curve was obtained *via* indirect Fourier transform of the scattering profile and was displayed as the pair distance distribution function $p(r)$ (Fig. 1*c*). The $p(r)$ value of $RseA_{169–186}$ exhibits a maximum dimension ($D_{max}$) of 7.10 nm, indicating that the $RseA_{169–186}$ fragment has an extended conformation in solution, as shown in the above Kratky analysis. In agreement with the SAXS scattering data, the CD spectra of the RseA fragments (Figs. 2*a* and 2*b*) imply that it adopts a random-coiled structure with minimum ellipticity near 200 nm, thereby supporting the notion that the RseB binding region ($RseA_{169–196}$) is unstructured when it is not bound. In addition, the solution SAXS (Fig. 1) and CD data (Fig. 2*c*) both support the premise that $RseA_{121–216}$ has a random structure.

The $p(r)$ function of RseB exhibits a bimodal pattern with a $D_{max}$ of 17.70 nm (Kim *et al.*, 2007 and Table 1). The $RseA_{169–196}$/RseB complex shows a similar pattern with two peaks, and the tail is somewhat shortened ($D_{max}$ = 16.30 nm) when compared with RseB, thereby indicating that slight structural alterations have occurred upon the formation of the complex (Fig. 1*c* and Table 1). The molecular shape models, calculated from the scattering curves of RseB and $RseA_{169–196}$/RseB, more clearly show the structural changes in RseB induced by the RseA binding (Figs. 3*a* and 3*b*). In the $RseA_{169–196}$/RseB structure, the large domain of each subunit appears to be rotated clockwise along the twofold symmetry axis. These results indicate that even the binding of the short minimal binding motif induces the conformational changes of RseB. The structural transformation in the dimer interface is clearly seen in $RseA_{121–216}$/RseB (Fig. 3*c*). On the other hand, the $p(r)$ function of the $RseA_{121–216}$/RseB complex shows a single peak pattern, which is characteristic of compact globular proteins, with a $D_{max}$ of 13.70 nm (Fig. 1*c*). Thereby the model structure also implies a compact structure in which the groove of the RseB dimer is filled (Fig. 3*c* and Kim *et al.*, 2007). Therefore the structural transformation is more obviously observed in the main body of $RseA_{121–216}$/RseB than in $RseA_{169–196}$/RseB.

Notably, the conformation of RseA appears to become altered upon the binding of RseB. It is possible that $RseA_{169–186}$ has acquired helical properties to some extent when it is complexed with RseB, because the CD spectrum of $RseA_{169–186}$ obtained by subtracting the CD spectrum of RseB from that of $RseA_{169–186}$/RseB shows a double minimum near 204 and 225 nm, and a maximum at 190 nm, which are characteristic of helical contents (Fig. 2*d*). Additionally, the difference between the CD spectrum of free RseB and that of the $RseA_{121–216}$/RseB complex is not identical to that of free $RseA_{121–216}$,

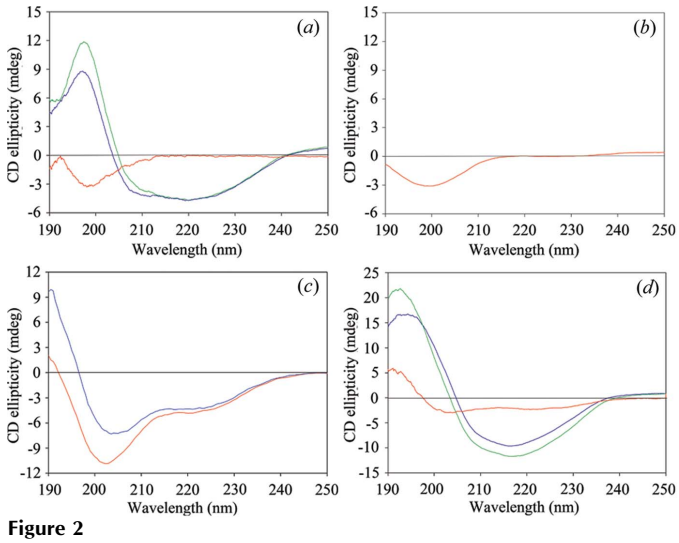


**Figure 2**
CD spectra of RseA in the absence or presence of bound RseB. (*a*) Calculated CD spectrum of $RseA_{169–186}$ (red) generated by subtracting the spectrum of His–Trx (green) from that of His–Trx–$RseA_{169–186}$ (blue). The CD spectrum indicates that the RseB binding motif of RseA is random coiled in solution. (*b*) CD spectrum of synthesized $RseA_{169–186}$ peptide. It shows a similar pattern to the calculated CD spectrum of $RseA_{169–186}$. (*c*) CD spectra of the periplasmic domain of RseA ($RseA_{121–216}$) in free (red) and bound (light blue) states, which is obtained by subtracting the spectrum of free RseB from that of $RseA_{121–216}$/RseB. (*d*) Calculated CD spectrum of $RseA_{169–186}$ (red) generated by subtracting the spectrum of free RseB (blue) from that of the $RseA_{169–186}$/RseB complex (green). This spectrum shows the presence of helical components, thereby suggesting that the RseB binding motif of RseA might have acquired some helical properties upon RseB binding.

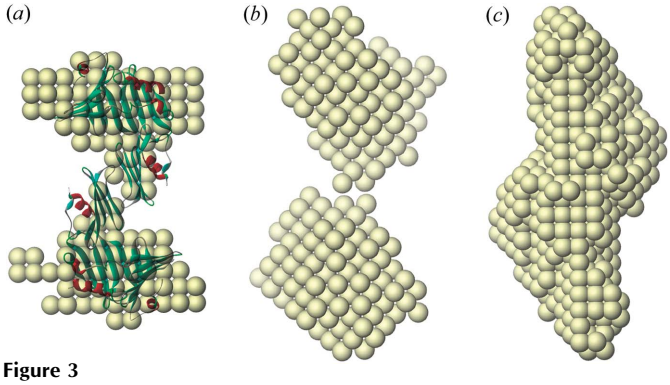


**Figure 3**
Solution models of (*a*) RseB, (*b*) the $RseA_{169–196}$/RseB complex and (*c*) the $RseA_{121–216}$/RseB complex obtained from SAXS data. The SAXS models are represented by dummy balls using *Discovery Studio 1.6* (Accelrys Inc., San Diego, CA, USA) in the same scale. The ribbon diagram of the RseB dimer is superimposed onto the solution model of RseB.

implying that $RseA_{121–216}$ might have different conformations in the free and the bound states (Fig. 2*c*). However, the discrepancy between the measured CD spectrum of free RseAs and the calculated CD spectrum obtained using the spectra of $RseA_{169–186}$ or $RseA_{121–216}$ in complex might not represent the conformational changes of RseAs, but originate from some changes in the secondary structure of RseB. At least, it is obvious that RseA binding to RseB causes conformational changes, in either RseA, RseB or both, since the CD spectrum of the complex is not the simple summation of the spectra of RseA and RseB. It can be assumed that these conformational changes are related to the regulation of RseA cleavage.

### 3.3. Implications of the RseA binding to RseB and their conformational changes

The sequential digestion of RseA in periplasmic and cytoplasmic spaces mediated by DegS and RseP, respectively, results in the release of bound $\sigma^E$ for the activation of the stress responsive genes (Alba & Gross, 2004). In this process, RseB plays an essential role in the fine tuning of envelope stress signalling *via* the modulation of the cleavage of RseA mediated by both RseP and DegS (Grigorova *et al.*, 2004; Cezairliyan & Sauer, 2007). In addition to our previous crystallographic and SAXS studies on RseB and its complex with RseA (Kim *et al.*, 2007), we performed CD and further SAXS experiments using various RseA fragments, in unbound and complexed states, to investigate the mechanism inherent to the regulation of RseA cleavage by RseB in structural aspects.

The SAXS and CD data suggest that the minimum RseB binding fragment and the whole periplasmic domain of RseA are highly unstructured in the free state (Figs. 1 and 2). RseB was expected to have structural flexibility to some extent, since it forms a loosely packed dimer and the solution SAXS and crystal models were similar but not identical (Fig. 3*a*) (Kim *et al.*, 2007). It appears that the RseA binding causes conformational changes in both fragments and results in the formation of a stable complex (Fig. 3). Whereas $RseA_{169–196}$, the minimum binding region required for RseB binding, causes limited local changes in RseB (Fig. 3*b*), conformational changes seem to be wider upon the binding of $RseA_{121–216}$ (Fig. 3*c*). In the overall structure, the large domain of each subunit of RseB appears to be rotated clockwise along the twofold symmetry axis. Interestingly, in the solution SAXS model of the $RseA_{169–196}$/RseB complex, the position of the RseA fragment could not be clearly identified, although it was obviously bound to RseB and induced conformational changes in RseB (Fig. 3*b*). However, the solution model of $RseA_{121–216}$/RseB clearly shows that its envelope is more globular than either free RseB or the $RseA_{169–196}$/RseB complex, thereby suggesting that the cleft in free RseB is occupied by a certain region of RseA. Since the minimum binding fragment ($RseA_{169–196}$) was not clearly visualized in the $RseA_{169–196}$/RseB complex and the empty cleft in free RseB was occupied in the complex of $RseA_{121–216}$/RseB, it is thought that some other region of RseA was also involved in RseB binding and was visualized in the SAXS model of the $RseA_{121–216}$/RseB complex. Taking these results together, it can be proposed that the unstructured free RseA becomes more structured and stabilized when it binds to RseB, and more than two separate regions of RseA are involved in RseB binding. Consistently with our notion, it has been proposed that the periplasmic domain of RseA would interact with RseB using two regions: residues near 169–186 and an undefined region (Cezairliyan & Sauer, 2007; Kim *et al.*, 2007). Thus the interaction between RseA and RseB is likely to induce conformational changes of RseA into a more compact and ordered form.

Generally, unstructured peptides are good substrates of proteases, but become more resistant to proteolysis when they are ordered in a complex. RseA can be less susceptible to proteolytic digestion by RseP when it is complexed with RseB. This assumption can explain why the cytoplasmic fragment of RseA was released by RseP in RseB-knockout cells (Grigorova *et al.*, 2004). In the periplasmic space, the peptide bond between V148 and S149 of RseA is cleaved by DegS (Walsh *et al.*, 2003), and, in a similar way, RseB-bound RseA might be less flexible and less accessible to DegS than free RseA. It was recently reported that RseB binding restricts the digestion RseA by DegS (Cezairliyan & Sauer, 2007), and our findings are consistent with this notion. These studies clearly indicate the conformational changes of both RseA and RseB induced by their interaction. Regarding the role of RseB in regulating the cleavage of RseA, it can be proposed that the RseB binding does not simply block the access of RseP to RseA, but also renders the conformation of RseA more resistant to proteolytic actions.

This work was supported by the Korea Science and Engineering Foundation (KOSEF, National Research Laboratory Program and Center for Integrated Molecular Systems) (to MR), the 21C Frontier Functional Proteomics Program (FPR06B2-120), the Ubiquitome Research Program (M10533010001-05N3301-00100) and the National Research Laboratory Program (NRL-2006-02287) of the Korea Ministry of Science and Technology (to KKK).

## References

Alba, B. M. & Gross, C. A. (2004). *Mol. Microbiol.* **52**, 613–619.
Alba, B. M., Leeds, J. A., Onufryk, C., Lu, C. Z. & Gross, C. A. (2002). *Genes Dev.* **16**, 2156–2168.
Bolze, J., Kim, J., Huang, J.-Y., Rah, S., Youn, H. S., Lee, B., Shin, T. J. & Ree, M. (2002). *Macromol. Res.* **10**, 2–12.
Cezairliyan, B. O. & Sauer, R. T. (2007). *Proc. Natl Acad. Sci. USA*, **104**, 3771–3776.
Flanagan, J. M., Kataoka, M., Shortle, D. & Engelman, D. M. (1992). *Proc. Natl Acad. Sci. USA*, **89**, 748–752.
Flynn, J. M., Levchenko, I., Sauer, R. T. & Baker, T. A. (2004). *Genes Dev.* **18**, 2292–2301.
Glatter, O. (1982). *Small Angle X-ray Scattering*, edited by O. Glatter & O. Kratky, pp. 119–196. London: Academic Press.
Grigorova, I. L., Chaba, R., Zhong, H. J., Alba, B. M., Rhodius, V., Herman, C. & Gross, C. A. (2004). *Genes Dev.* **18**, 2686–2697.
Jang, D. S., Lee, H. J., Lee, B., Hong, B. H., Cha, H. J., Yoon, J., Lim, K., Yoon, Y. J., Kim, J., Ree, M., Lee, H. C. & Choi, K. Y. (2006). *FEBS Lett.* **580**, 4166–4171.
Kanehara, K., Ito, K. & Akiyama, Y. (2002). *Genes Dev.* **16**, 2147–2155.
Kataoka, M., Hagihara, Y., Mihara, K. & Goto, Y. (1993). *J. Mol. Biol.* **229**, 591–596.
Kataoka, M., Nishii, I., Fujisawa, T., Ueki, T., Tokunaga, F. & Goto, Y. (1995). *J. Mol. Biol.* **249**, 215–228.
Kim, D. Y., Jin, K. S., Kwon, E., Ree, M. & Kim, K. K. (2007). *Proc. Natl Acad. Sci. USA*, **104**, 8779–8784.
Missiakas, D., Mayer, M. P., Lemaire, M., Georgopoulos, C. & Raina, S. (1997). *Mol. Microbiol.* **24**, 355–371.
Rhodius, V. A., Suh, W. C., Nonaka, G., West, J. & Gross, C. A. (2006). *PLoS Biol.* **4**, e2.
Roe, R.-Y. (2000). *Methods of X-ray and Neutron Scattering in Polymer Science.* Oxford University Press.
Semenyuk, A. V. & Svergun, D. I. (1991). *J. Appl. Cryst.* **24**, 537–540.
Svergun, D. I., Petoukhov, M. V. & Koch, M. H. J. (2001). *Biophys. J.* **80**, 2946–2953.
Volkov, V. V. & Svergun, D. I. (2003). *J. Appl. Cryst.* **36**, 860–864.
Walsh, N. P., Alba, B. M., Bose, B., Gross, C. A. & Sauer, R. T. (2003). *Cell*, **113**, 61–71.
Wilken, C., Kitzing, K., Kurzbauer, R., Ehrmann, M. & Clausen, T. (2004). *Cell*, **117**, 483–494.
Yu, C.-J., Kim, J., Kim, K.-W., Kim, G.-H., Lee, H.-S., Ree, M. & Kim, K.-J. (2005). *J. Korean Vac. Soc.* **14**, 138–142.